Volume 66, Issue 1   JUNE 2012   ISSN 0032-0633

Special Issue:
Rosetta Fly-by at Asteroid (21) Lutetia
Guest Editors: R. Schulz and C. Alexandar

ELSEVIER

PLANETARY and SPACE SCIENCE

Possible evidence for partial differentiation of asteroid Lutetia from Rosetta

Benjamin P. Weiss [a],*, Linda T. Elkins-Tanton [a], M. Antonietta Barucci [b], Holger Sierks [c], Colin Snodgrass [c], Jean-Baptiste Vincent [c], Simone Marchi [d], Paul R. Weissman [e], Martin Pätzold [f], Ingo Richter [g], Marcello Fulchignoni [b], Richard P. Binzel [a], Rita Schulz [h]

[a] Department of Earth, Atmospheric, and Planetary Sciences, Massachusetts Institute of Technology, Cambridge, MA, USA
[b] Observatoire de Paris LESIA, France
[c] Max Planck Institute for Solar System Research, Katlenburg-Lindau, Germany
[d] Departement Cassiopée, Université de Nice-Sophia Antipolis, Observatoire de la Côte d'Azur, CNRS, France
[e] Planetary Ices Section, Jet Propulsion Laboratory, Pasadena, CA, USA
[f] Rheinisches Institut für Umweltforschung, Abt. Planetenforschung, an der Universität zu Köln, Cologne, Germany
[g] TU-Braunschweig, Institute for Geophysics and Extraterrestrial Physics, Braunschweig, Germany
[h] European Space Agency, Research and Scientific Support Department, Noordwijk, Netherlands

ARTICLE INFO

ABSTRACT

The petrologic diversity of meteorites demonstrates that planetesimals ranged from unmelted, variably metamorphosed aggregates to fully molten, differentiated bodies. However, partially differentiated bodies have not been unambiguously identified in the asteroid belt. New constraints on the density, composition, and morphology of 21 Lutetia from the Rosetta spacecraft indicate that the asteroid's high bulk density exceeds that of most known chondritic meteorite groups, yet its surface properties resemble those of some carbonaceous and enstatite chondrite groups. This indicates that Lutetia likely experienced early compaction processes like metamorphic sintering. It may have also partially differentiated, forming a metallic core overlain by a primitive chondritic crust.

1. Introduction

Chondritic meteorites are aggregates of primitive materials formed in the solar nebula. However, it has long been known that nearly all chondrites experienced varying degrees of postaccretional aqueous alteration and thermal metamorphism on their parent planetesimals (Anders, 1964). These processes led to textural, chemical and mineralogical changes that form the basis of a petrologic classification scale (types 1–7) that reflects increasing degrees of thermal equilibration (types 3–7) (Huss et al., 2006) and aqueous alteration (types 1–2) (Brearley, 2006). The heat sources that drove these processes were most likely short-lived radionuclides (Hevey and Sanders, 2006; Huss et al., 2006) and, to some extent, meteoroid impacts (Davison et al., 2010; Keil et al., 1997; Rubin, 2004). Thermal modeling of asteroid metamorphism from radionuclide decay has motivated the onion shell model in which the planetesimal's interior forms a radially layered structure with a highly metamorphosed deep interior overlain by progressively less heated outer layers. However, despite the ubiquitous meteoritic evidence for thermal metamorphism, it has been difficult to identify evidence for this process on extant asteroids. A key difficulty is the lack of detailed in situ observations of bodies that are sufficiently large to retain their large-scale structures intact from the early solar system.

A second longstanding problem in asteroid science is that the great majority of known meteorite parent bodies melted and formed metallic cores, but very few differentiated asteroids have been identified in the asteroid belt (Burbine et al., 2002). Three possible explanations for this discrepancy are that the meteorite suite is not representative of the present-day asteroid belt (Burbine et al., 2002), that few differentiated asteroids have survived to the present day (Bottke et al., 2006), or that some asteroid spectral classes typically associated with chondritic bodies also contain differentiated members (Gaffey et al., 1993a). A fourth possibility is that partially differentiated asteroids, with metallic cores and partially or totally melted mantles

* Corresponding author. Tel.: +1 617 324 0224.
E-mail address: bpweiss@mit.edu (B.P. Weiss).

overlain by unmelted chondritic crusts, formed in the early solar system (Carporzen et al., 2011; Elkins-Tanton et al., 2011; Sahijpal and Gupta, 2011; Weiss et al., 2010) and are extant but undiscovered in the asteroid belt. However, the latter scenario is at odds with the traditional view that chondrites, whose aggregational textures require that they never melted, formed on smaller and/or younger bodies that never differentiated.

Large-scale melting of rocky asteroids is thought to have been driven by heating from short-lived radionuclides on bodies larger than ~10–30 km in radius that accreted within ~1.5–2 million years (Ma) after the formation of calcium aluminum inclusions (CAIs) (Elkins-Tanton et al., 2011; Hevey and Sanders, 2006; Sahijpal et al., 2007; Sahijpal and Gupta, 2011). With triaxial ellipsoid dimensions of ~126 × 103 × 95 km³ (Sierks et al., in press), 21 Lutetia is the first asteroid unambiguously in the size regime capable of large-scale melting and metallic core formation to be visited by a spacecraft. The next two largest asteroids previously encountered, 253 Mathilde and 243 Ida, have mean radii of 26.5 and 15.7 km, respectively (Davis, 1999; Thomas et al., 1996; Veverka et al., 1997). Asteroids with radii greater than ~20–30 km have collisional lifetimes (e.g., mean time between impacts capable of breaking an asteroid into fragments whose largest piece has a mass less than half of the parent asteroid) greater than the age of the solar system (Bottke et al., 2005; Marchi et al., 2006). Therefore, Lutetia is also the first asteroid visited by a spacecraft that is of sufficient size to have potentially retained most of its original large scale structure against impact disruption. This means that Lutetia may have retained a mostly intact record of any early metamorphic and melting processes. Whether Lutetia actually melted, was just thermally metamorphosed, or remained unheated would have depended predominantly on when it began to accrete and on its initial composition. Here we use recent Rosetta observations, ground-based astronomical measurements, and meteorite data to demonstrate that Lutetia experienced at least large scale thermal metamorphism and possibly even partial differentiation and core formation.

2. Composition of Lutetia's surface

The composition and nature of Lutetia have long been perplexing (Barucci and Fulchignoni, 2009). Ground-based visible-near-infrared reflectance spectra and new infrared spectra from VIRTIS onboard Rosetta (Coradini et al., in press) are flat and nearly featureless [spectral class Xc (Demeo et al., 2009)], compatible with some carbonaceous chondrites (Belskaya et al., 2010; Birlan et al., 2006) and enstatite chondrites (Ockert-Bell et al., 2010) but distinct from all other meteorite groups with the possible exception of iron meteorites (Cloutis et al., 2010). Some Lutetia spectra (Birlan et al., 2006) show a weak ~1 μm absorption feature like that observed for some carbonaceous chondrites (Clark et al., 2009; Gaffey, 1976) and enstatite chondrites (Gaffey, 1976), although this feature is not present in many other spectra including that of VIRTIS (Coradini et al., in press).

The mean visible geometric albedo measured by the OSIRIS camera onboard Rosetta is 0.19 ± 0.01. This is consistent with bidirectional reflectance measurements of enstatite chondrites (Ockert-Bell et al., 2010). Although it has been suggested that Lutetia's visual geometric albedo is too high to be consistent with carbonaceous chondrites (Vernazza et al., 2009), the reflectance of CK, CO, CR, and CV chondrites are actually known to range from 0.5 to 0.22 (Chapman and Salisbury, 1973; Clark et al., 2009; Gaffey, 1976). Because laboratory experiments have typically either measured the bidirectional reflectance at phase angles larger than 5–10° [e.g., Clark et al. (2002)] or else the directional-hemispherical reflectance [e.g., Clark et al. (2009)], such

experiments should place lower limits on the inferred geometric albedo (which is defined at zero phase angle) due to the opposition effect. Using the phase function for Lutetia determined by OSIRIS observations (Sierks et al., in press), the asteroid's mean albedo is in fact only 0.13 at a phase angle of 5° and much lower at higher phase angles (Coradini et al., in press). Therefore, as pointed out by Drummond et al. (2010), Lutetia's geometric albedo is in agreement with high-albedo (CO, CK, and probably CV and CR) carbonaceous chondrites as well as enstatite chondrites (Fig. 1).

Lutetia's polarization properties differ from those of all other measured asteroids but are distinctively similar to CV and CO chondrites and different from other chondrite groups as well as all known achondrites (Belskaya et al., 2010). Moreover, Spitzer Space Telescope 8–38 μm emissivity spectra of Lutetia show a clear Christiansen peak at 9.3 μm that is typical of CO and CV carbonaceous chondrites (Barucci et al., 2008) and differs from that of enstatite and ordinary chondrites and stony achondrites (whose Christiansen peaks are known to range from 8.3–8.9 μm) (Izawa et al., 2010; Salisbury et al., 1991). The lack of a deep 3 μm absorption for much of Lutetia's surface (Barucci and Fulchignoni, 2009; Coradini et al., in press) does not favor a connection with hydrated carbonaceous chondrites (CI, CM, CR, CH, and CB) [although the other face of Lutetia that was not visible to Rosetta may show this hydration feature (Rivkin et al., 2011)]. Finally, two measurements of the OC radar albedo of Lutetia obtained values of 0.19 ± 0.07 (Magri et al., 1997) and 0.24 ± 0.07 (Shepard et al., 2010) (1σ uncertainties), implying bulk regolith densities of 1900–2900 and 2300–3300 kg m⁻³, respectively [using equation (8) from Shepard et al., 2010)]. Assuming 40–50% regolith total porosity, the radar measurements of Magri et al. (1997) and
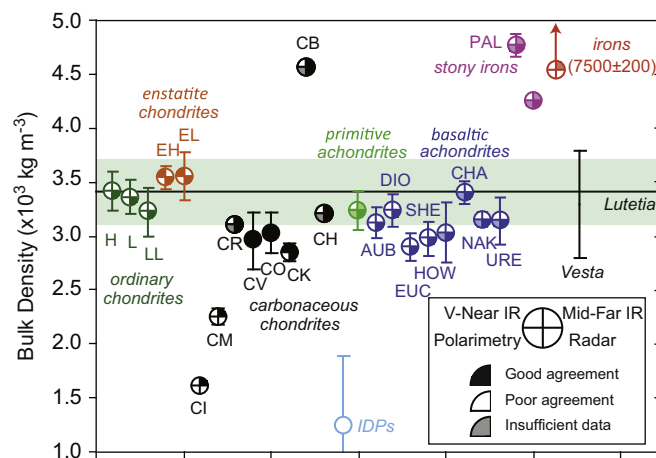

Fig. 1. Measured mean bulk densities and surface observational properties of various meteorite groups as compared to those of asteroid 21 Lutetia (Pätzold et al., in press; Sierks et al., in press). Vertical position of each circular symbol gives bulk density, while quadrants in each symbol denote agreement with four different compositional constraints on the surface of Lutetia: top-left=visible to near infrared reflectance spectra (0.5–3.0 μm) (best studied constraint), top-right=mid-far infrared reflectance spectra (>3 μm), bottom-left=visible polarimetry, and bottom-right=OC radar-albedo (second best studied constraint). IDPs=interplanetary dust particles (unmelted chondritic), AUB=aubrites, DIO=diogenites, EUC=eucrites, HOW=howardites, SHE=shergottites, CHA=chassignites, NAK=nakhlites, URE=ureilites, PAL=pallasites, MES=mesosiderites. Meteorite classes (ordinary chondrites, basaltic achondrites, etc.) are arranged along vertical axis approximately by petrologic similarity. The density of Vesta is shown for comparison (mean value given by black line and uncertainty range shown in green). Data and references for the density and surface composition measurements are presented in Tables 2 and 4, respectively. Error bars give measured one standard deviation variance of meteorites within each group when known (for exceptions and details, see Table 2). The bulk densities shown here should not be compared to the lower grain densities used to estimate the regolith composition from radar albedo measurements (see Section 2).

Shepard et al. (2010) imply grain densities ranging from 3167–5800 and 3833–6600 kg m^{-3}, respectively. The total density range spanned by these two measurements is consistent with a porous regolith composed of carbonaceous (e.g., CO, CV, CK, CR, CH, CB), ordinary, and enstatite chondrites, as well as basaltic, primitive, and stony iron achondrites, but inconsistent with an iron meteorite and CM and CI carbonaceous chondrite composition (Consolmagno et al., 2008). In summary, Lutetia's surface is unambiguously not a pure composition of known ordinary chondritic, basaltic achondritic, or iron meteoritic materials. Rather, current constraints favor a primitive surface similar to that of CV, CO, and CK carbonaceous chondrites, although an enstatite chondrite composition cannot be ruled out (Fig. 1). As we will see below, our conclusions about the nature of Lutetia's interior are robust for either CV/CO/CK carbonaceous or enstatite chondrite surface compositions, both of which indicate a primordial, unmelted chondritic crust.

3. Constraints on interior of Lutetia

There are no unambiguous exposures of bedrock or variegated interior compositional units visible in OSIRIS images (Sierks et al., in press) and VIRTIS spectral maps (Coradini et al., in press). The nature of Lutetia's interior must therefore be constrained indirectly using gravity, shape, and magnetic data. The Rosetta OSIRIS and RSI experiments have now determined that Lutetia has a bulk density of 3400 ± 300 kg m^{-3} (Pätzold et al., in press; Sierks et al., in press). This is among the largest densities known for any asteroid and within error of that of the differentiated asteroid 4 Vesta (Kuzmanoski et al., 2010) and the X-type asteroid 22 Kalliope (Decamps et al., 2008).

The two Rosetta magnetometers RPCMAG and ROMAP found that the magnetic field of Lutetia was less than 1 nT at the closest approach distance of ~3170 km (Richter et al., in press). Following Baumgartel et al. (2007) and Simon et al. (2006), this indicates that the net dipole moment of the asteroid must be $< 10^{12}$ Am^2 (Richter et al., in press). If we assume a uniform magnetization throughout the asteroid, this would indicate a maximum magnetization of 6×10^{-7} Am^2 kg^{-1}. However, if the fine-scale magnetization of Lutetia is not unidirectional, as expected for the product of an internally generated field (Runcorn, 1975), its intensity could be orders of magnitude stronger than this value. Given that the natural remanent magnetizations of small body stony, stony iron, and iron meteorites range between $\sim 10^{-1}$ and 10^{-5} Am^2 kg^{-1} (Auster et al., 2010), it is not possible to establish from these data whether Lutetia has substantial fine-scale remanent magnetization like that expected from an internal core dynamo (Weiss et al., 2008) or externally generated fields in the early solar system (Weiss et al., 2010).

Lutetia's bulk density can be compared to the densities of meteorite groups to constrain its bulk composition under the assumption that the known meteorite suite is broadly representative of asteroid compositions. Its bulk density equals or exceeds both the bulk densities and the grain densities of all known meteorite groups with the exception of iron and stony iron meteorites and the rare CB carbonaceous chondrite group (Fig. 1). A pure composition of any of the latter three lithologies is in any case inconsistent with Lutetia's visible-near infrared spectral properties (Gaffey, 1976; Hiroi et al., 1993; Osawa et al., 2005) (Fig. 1). [Note that although it is more conservative to compare Lutetia's bulk density to meteorite grain densities rather than meteorite bulk densities, such an approach is in fact overly restrictive because the overburden pressure in Lutetia should reach only 4 MPa even in the center of the asteroid—see equation (7) in Asphaug et al. (2002)—which is below the brittle compressive strength of essentially all measured meteorites except for some CI and CM chondrites and the most friable meteors (Svetsov et al., 1995; Tsuchiyama et al., 1998; Petrovic, 2001). Therefore, meteorite bulk densities would not be significantly reduced by overburden pressures in Lutetia relative to laboratory measurements.] Given the uncertainty range for Lutetia's bulk density, if the asteroid has more than ~13% macroporosity (presumably from large scale fracturing or brecciation), then the bulk densities of its constituent materials would exceed the mean bulk densities of all known chondrite, basaltic, and primitive achondrite meteorite groups excluding CB chondrites.

In fact, there is indirect evidence that Lutetia has substantial macroporosity. Its thermal inertia of 10–30 J K^{-1} m^{-2} s$^{-1/2}$ (Coradini et al., in press; Gulkis et al., submitted for publication; Sierks et al., in press) implies that at least its surface layer has dusty regolith-like porosities ($> 40\%$). The regolith imaged by OSIRIS has a thickness up to ~600 m around the crater in the Baetica region (Sierks et al., in press). Because this regolith layer is unlikely to be representative of most of Lutetia's volume, other more indirect constraints are necessary to constrain the porosity of the interior. Firstly, the observed crater size frequency distribution suggests that a ~3 km thick fractured surface layer overlies more competent rock in the Achaia region (Sierks et al., in press). Secondly, estimates of local slopes on Lutetia (angle between surface normal and net acceleration vector from gravity and rotation) derived from OSIRIS images (Sierks et al., in press) find that only 5% of the surface is steeper than 33° (approximately the maximum angle of repose of sand) and only 0.1–1% of the surface is steeper than 40–50° (the angle of repose for talus and poorly sorted angular fragments) (Fig. 2). This compares with values of ~3–4% and 2%, respectively for Eros (Asphaug et al., 2002). Like Eros, Lutetia's low slopes are consistent with a body whose outer layer is mostly strengthless at large scales. More importantly, scaling laws indicate that the minimum diameters of hypervelocity impactors that would catastrophically destroy and shatter Lutetia are ~22 km and ~1.6–3.8 km, respectively [see Holsapple (2009) and Table 1]. Using scaling laws for hard rock and assuming an impact in the strength regime, the bolide which formed the largest crater visible in OSIRIS images of Lutetia [which has a diameter of ~55 km (Sierks et al., in press)] would have a diameter of ~7.2–11.2 km [see Holsapple and Housen

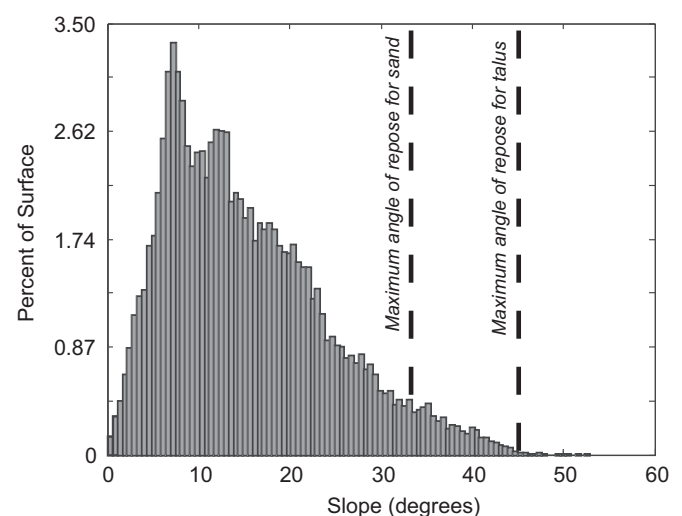**Fig. 2.** Histogram of slopes (angle between surface normal and local gravitational acceleration vector) on Lutetia. Shown is the percentage of the surface with slope values within a given bin. The slopes were calculated using the OSIRIS-determined shape model and assuming a uniform density equal to that of the bulk asteroid. Shown for comparison are typical angles of repose for sand and poorly sorted, angular fragments (talus).

Table 1
Parameters used to estimate cratering effects on Lutetia.

Parameter	Values	Reference
Average diameter of target	98.4 km	(Sierks et al., in press)
Density of target	3400 kg m^{-3}	(Pätzold et al., in press; Sierks et al., in press)
Specific energy for disruption, Q_D^*[1]	8×10^4 J kg^{-1}	(Bottke et al., 2005)
Specific energy for shattering, Q_S^*[1]	30–400 J kg^{-1}	(Holsapple, 2009)
Projectile density[2]	2600 kg m^{-1}	(Consolmagno et al., 2008)
Impactor relative velocity	4.3 km s^{-1}	(Marchi et al., 2010)
Angle of impact[3]	45°	(Gilbert, 1893)
Diameter of largest visible crater on target	55 km	(Sierks et al., in press)
Strength of target[4]	1–5×10^7 Pa	(Asphaug et al., 1996)

[1] If Lutetia has a substantial metallic core, these values could underestimate Q_D^* and Q_S^*. Unfortunately, we are unaware of any published estimates of these parameters for differentiated bodies. However, because Lutetia is likely sufficiently large to be in the gravity regime for collisions, the dependence of Q_D^* and Q_S^* with material strength is probably modest relative to other uncertainties in this problem [see Fig. 14 of Ryan and Melosh (1998)]. Furthermore, in the context of our differentiation models, even a body fully melted out to 80% of its radius and bulk metal abundance at the upper end of all non-CB chondrite groups (15 vol. %) is expected to have a metallic core representing < 10 vol% of the body.
[2] Average density of S-type asteroids.
[3] Most probable angle of impact for an isotropic distribution of impactors. This was used for determining impactor diameter, which produced the largest crater on Lutetia. For the shattering and disruption calculations, Q_D^* and Q_S^* values were used that average over an isotropic distribution of impactors [see Benz and Asphaug (1999)] rather than for a single impact angle.
[4] Typical for bulk silicate rock. Note that even if Lutetia has a metallic core, only the strength of the surface (down to the approximate depth of the transient crater) is relevant for the estimate of the impactor size required to produce the largest crater.

Table 2
Bulk densities of meteoritic materials and asteroids 21 Lutetia and 4 Vesta (Fig. 1).

Meteorite group	Bulk density (kgm^{-3})	1σ (kgm^{-3})	Reference
H ordinary chondrites	3420	180	(Consolmagno et al., 2008)
L ordinary chondrites	3360	160	(Consolmagno et al., 2008)
LL ordinary chondrites	3220	220	(Consolmagno et al., 2008)
EH chondrites	3540	110	(Macke et al., 2010)
EL chondrites	3550	220	(Macke et al., 2010)
CI carbonaceous chondrites	1600	30	(Consolmagno et al., 2008)
CM carbonaceous chondrites	2250	80	(Consolmagno et al., 2008)
CR carbonaceous chondrites	3100	–	(Britt and Consolmagno, 2003)
CV carbonaceous chondrites	2960	260	(Consolmagno et al., 2008)
CO carbonaceous chondrites	3030	190	(Consolmagno et al., 2008)
CK carbonaceous chondrites	2850	80	(Consolmagno et al., 2008)
CB carbonaceous chondrites	4560	–	(Consolmagno et al., 2007)[1]
CH carbonaceous chondrites	3200	–	(Britt and Consolmagno, 2003)[1]
primitive achondrites	3230	180	(Consolmagno et al., 2008)
unmelted chondritic interplanetary dust particles (IDPs)	1100[2]	625[2]	(Flynn, 1994)
aubrites	3120	150	(Britt and Consolmagno, 2003)
diogenites	3230	150	(Consolmagno et al., 2008)
eucrites	2900	130	(Consolmagno et al., 2008)
howardites	2970	160	(Consolmagno et al., 2008)
shergottites	3030	280	(Consolmagno et al., 2008)
chassignites	3400	110	(Consolmagno et al., 2008)
nakhlites	3150	70	(Consolmagno et al., 2008)
ureilites	3140	220	(Consolmagno et al., 2008)
pallasites	4760	100	(Britt and Consolmagno, 2003)
mesosiderites	4250	20	(Britt and Consolmagno, 2003)
iron meteorites[3]	7500	200	(Britt et al., 2002)
asteroid 21 Lutetia	3400	300	(Pätzold et al., in press; Sierks et al., in press)
asteroid 4 Vesta	3300	500	(Kuzmanoski et al., 2010)

[1] The bulk densities of these meteorite groups are particularly poorly known. These values were each estimated from grain density measurements of a single meteorite and an assumed bulk density of 7%.
[2] Encompasses range of peak values in measured bimodal distribution [see Flynn (1994)].
[3] Typical value and range.

(2007) and Table 1]. If Lutetia has a metallic interior, then these would represent lower limits on the impactor size because they assume a pure silicate rock interior. Therefore, these calculations indicate that Lutetia should have at least a thoroughly fractured "brick pile" structure and possibly even be a shattered, reaccreted rubble pile [e.g., Housen (2009)], consistent with our estimation that the shattering lifetime for a body of Lutetia's size is likely less than the age of the solar system (Holsapple et al., 2002). This makes Lutetia similar to other asteroids previously visited by spacecraft, which also have abundant fractures and joints (Asphaug, 2009). These bodies were inferred to have macroporosities of ~ 6–40% (Consolmagno et al., 2008; Wilkison et al.,

2002), suggesting that Lutetia may have similarly substantial porosity. Furthermore, essentially all other asteroids of similar size to Lutetia ($< \sim 10^{20}$ kg), with the possible exception of 20 Massalia, are thought to have macroporosities of > 5–10% and ranging up to $\sim 80\%$ (Consolmagno et al., 2008).

A stringent upper limit on Lutetia's macroporosity of $\sim 52\%$ is provided by a model in which the entire asteroid below a very thin chondritic surface layer is made of pure iron. However, given that impact craters visible on Lutetia have excavated hundreds of meters to several kilometers deep into Lutetia, the lack of

Table 3
Parameters for Lutetia differentiation models (Fig. 3).

Parameter	Values	Reference
Planetesimal radius	50 km[1]	(Sierks et al., in press)
Fe metal abundance[2]	5, 10, 15, 20, 25, and 30 vol%	(Scott and Krot, 2005)
Core (Fe metal) material density[3]	7500 kg m^{-3}	(Britt et al., 2002)
Cumulate mantle silicate density[4]	3300 kg m^{-3}	(Consolmagno et al., 2008)
Porous crust total porosity	50%	(Elkins-Tanton et al., 2011; Hevey and Sanders, 2006; Sahijpal et al., 2007; Yomogida and Matsui, 1984)
Sintered crust total porosity[5]	7%	(Consolmagno et al., 2008)
Thickness of unmelted crust[6,7]	2–50 km	(Elkins-Tanton et al., 2011)
Additional macroporosity	10, 20%	

[1] This is likely a lower limit on Lutetia's post-accretional radius since the body has probably been subsequently reduced in size due to impacts.

[2] Chondrites other than CB, CR, and CH chondrites have metal abundances ranging from < 0.01 to 15 vol%.

[3] Typical for iron meteorites.

[4] Typical for basaltic achondrites.

[5] Typical for chondrites other than CM and CI carbonaceous chondrites, all of which have been heated to at least 200 °C (Cody et al., 2008; Huss et al., 2006).

[6] This can range widely depending on the time at which accretion initiates and its duration.

[7] The crustal density is calculated as $7500 \times (1 - \text{porosity}) \times (\text{metal volume fraction}) + 3300 \times (1 - \text{porosity}) \times (1 - \text{metal volume fraction})$, where 7500 and 3300 are the assumed densities of the metal and silicate fractions, respectively, in kg m^{-3}. This relation assumes that the metal and silicate portions of the crustal material are equally porous (probably not strictly correct but producing an insignificant error).

Table 4
Surface optical properties of meteorites and their comparison with Lutetia (Fig. 1)[1].

Meteorite Group	Visible-near IR	Mid-far IR	Polarimetry
H ordinary chondrites	(Clark et al., 2009; Gaffey, 1976)	(Salisbury et al., 1991)	(Belskaya et al., 2010)
L ordinary chondrites	(Clark et al., 2009)	(Salisbury et al., 1991)	(Belskaya et al., 2010)
LL ordinary chondrites	(Clark et al., 2009)	(Salisbury et al., 1991)	(Belskaya et al., 2010)
EH chondrites	(Clark et al., 2009)	(Izawa et al., 2010; Salisbury et al., 1991)	(Belskaya et al., 2010)
EL chondrites	(Clark et al., 2009)	(Izawa et al., 2010; Salisbury et al., 1991)	(Belskaya et al., 2010)
CI carbonaceous chondrites	(Clark et al., 2009)	(Lazzarin et al., 2009; Osawa et al., 2005; Salisbury et al., 1991)	(Belskaya et al., 2010)
CM carbonaceous chondrites	(Clark et al., 2009)	(Osawa et al., 2005; Salisbury et al., 1991)	(Belskaya et al., 2010)
CR carbonaceous chondrites	(Barucci and Fulchignoni, 2009; Clark et al., 2009; Izawa et al., 2010; Osawa et al., 2005)	(Osawa et al., 2005)	–
CV carbonaceous chondrites	(Clark et al., 2009)	(Osawa et al., 2005; Salisbury et al., 1991)	(Belskaya et al., 2010)
CO carbonaceous chondrites	(Clark et al., 2009)	(Lazzarin et al., 2009; Osawa et al., 2005; Salisbury et al., 1991)	(Belskaya et al., 2010)
CK carbonaceous chondrites	(Clark et al., 2009)	(Osawa et al., 2005; Salisbury et al., 1991)	(Geake and Dollfus, 1986)
CB carbonaceous chondrites	(Osawa et al., 2005)	(Osawa et al., 2005)	–
CH carbonaceous chondrites	(Osawa et al., 2005)	(Lazzarin et al., 2009; Osawa et al., 2005)	–
primitive achondrites	(Hiroi and Takeda, 1991; Hiroi et al., 1993)	–	–
IDPs	–	–	–
aubrites	(Vernazza et al., 2009)	(Salisbury et al., 1991)	(Belskaya et al., 2010; Geake and Dollfus, 1986; Lupishko and Belskaya, 1989)
diogenites	(Gaffey, 1976)	(Salisbury et al., 1991)	(Belskaya et al., 2010; Geake and Dollfus, 1986; Lupishko and Belskaya, 1989)
eucrites	(Gaffey, 1976)	(Salisbury et al., 1991)	(Geake and Dollfus, 1986)
howardites	(Gaffey, 1976)	(Salisbury et al., 1991)	(Belskaya et al., 2010; Geake and Dollfus, 1986; Lupishko and Belskaya, 1989)
shergottites	(Gaffey, 1976)	(Salisbury et al., 1991)	–
chassignites	(Gaffey, 1976; Pieters et al., 2008)	(Pieters et al., 2008)	–
nakhlites	(Dyar et al., 2005; Gaffey, 1976)	(Dyar et al., 2005)	–
ureilites	(Gaffey, 1976)	(Salisbury et al., 1991)	–
pallasites	(Hiroi et al., 1993)	–	–
mesosiderites	(Gaffey, 1976)	–	–
iron meteorites	(Cloutis et al., 2010; Gaffey, 1976)	–	(Belskaya et al., 2010)

[1] For references on meteorite bulk densities see Table 1. For constraints on the density of Lutetia's surface from radar, see discussion in text, Magri et al. (1997) and Shepard et al. (2010).

exposures of differentiated rocks suggests that the chondritic crust is likely at least several kilometers thick. For such a body with an enstatite or non-CB/CH carbonaceous chondrite-like bulk metal content, a more realistic upper limit on the macroporosity is ~25% (see Section 4.2).

4. Implications for interior structure and evolution of Lutetia

Lutetia's high bulk density and chondritic surface composition have major implications for the thermal evolution of the asteroid. A critical constraint is that Lutetia's large scale radial structure could have remained mostly intact since it formed. This is indicated by the 3.6 ± 0.1 Ga crater retention age for Lutetia's Achaia region (Sierks et al., in press, Marchi et al., submitted for publication) and the fact that the collisional lifetime of Lutetia is well in excess of the age of the solar system [following Bottke et al. (2005) and Marchi et al. (2006)]. Furthermore, given that Lutetia's macroporosity is likely $< \sim 25\%$ (see Sections 3 and 4.2), it is unlikely to have a rubble pile structure. Therefore, although Lutetia's nonspherical shape may be the product of several major collisions, the asteroid mostly may have preserved its original large-scale structure. Using this conclusion, we next argue that the data collectively provide strong evidence for at least thermal metamorphism (Section 4.1) and possibly even large-scale melting in the interior (Section 4.2).

4.1. Evidence for thermal metamorphism

The constituents of chondrites are generally thought to have accreted as relatively fine, dusty aggregates that progressively grew to form high porosity ($>30\%$) planetesimals (Bland et al., 2011; Ghosh et al., 2006; Hevey and Sanders, 2006; McSween et al., 2002; Sahijpal et al., 2007; Weidenschilling and Cuzzi, 2006). These porosities are greater than the mean porosities

measured for chondrite groups, which range from ~7–25% (Consolmagno et al., 2008). Sintering from post-accretional thermal metamorphism to >200–$300\,^\circ$C (Cody et al., 2008; Huss et al., 2006; Yomogida and Takafumi, 1983; Yomogida and Matsui, 1984) is thought to have been one of the dominant processes in ultimately reducing the microporosity of meteorite parent bodies to the low levels presently observed in chondrite groups. Only CI and CM chondrites, which have experienced the lowest levels of thermal metamorphism ($<150\,^\circ$C) (Cody et al., 2008), have bulk porosities approaching the levels expected in primordial planetesimals.

As discussed in Section 3, compaction due to overburden pressures on Lutetia is unlikely to influence its macroporosity (given that proto-Lutetia should not have been much more massive than present-day Lutetia). On the other hand, early impacts, which should have locally produced pressures exceeding the compressive strengths of many ordinary and carbonaceous chondrites (Weidenschilling and Cuzzi, 2006), would also have inevitably compacted an early, porous asteroid via fracturing and probably also some melting [see also Consolmagno and Britt (2004) and Sugiura and Strangway (1983)]. Although it is difficult to quantify the effects of impacts, they seem to be most efficient at compacting meteoritic materials with porosities $> \sim 30\%$ (Housen and Holsapple, 2003), suggesting that this is reasonably a lower limit on Lutetia's porosity prior to any metamorphism and aqueous alteration.

Despite the ubiquitous effects of the sintering process on chondrite groups, nearly all asteroids with chondrite-like surfaces [with the possible exception of 20 Massalia (Britt et al., 2002) and 22 Kalliope (Decamps et al., 2008)] are thought to have much higher total porosities than their meteorite analogs. This is almost certainly because meteoroid impacts have produced substantial post-accretional macroporosity in these bodies in the form of fracturing and/or brecciation. Therefore, it has been difficult to positively identify the effects of thermal metamorphism and
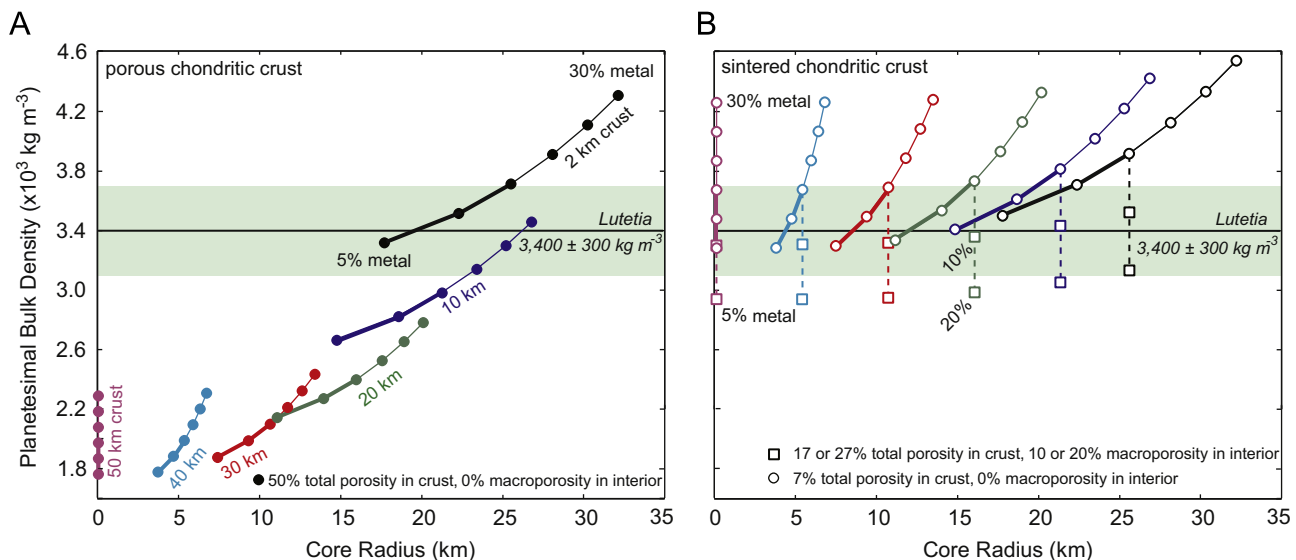

Fig. 3. Predicted bulk density for a 50 km radius spherical planetesimal as a function of the amount of melting and differentiation. The body is assumed to have an unmelted crust that has a total porosity of either 50% (A) or 7% (B) (representative of sintered and unsintered chondritic material, respectively) overlying a doubly layered differentiated interior (silicate mantle and iron metal core) with zero macroporosity. The crustal density is calculated as $7500 \times (1\text{-porosity}) \times (\text{metal volume fraction}) + 3300 \times (1\text{-porosity}) \times (1\text{-metal volume fraction})$, where 7500 and 3300 are the assumed densities of the metal and silicate fractions, respectively, in kg m^{-3}. This relation assumes that the metal and silicate portions of the crustal material are equally porous (probably not strictly correct but producing an insignificant error). Each curve represents a particular assumed unmelted crust thickness (specified below the curve), with individual points corresponding to a particular iron metal abundance (ranging from 5–50 vol%). Also shown in (B) is the predicted bulk density assuming macroporosity of 10% and 20% (additional to the crustal porosity described above) distributed uniformly throughout the entire volumes of bodies with sintered crusts and 15% vol% metal (squares). No pressure effects on density are included in these calculations due to the low pressures expected in Lutetia. Also, explicit variations in iron sulfide and iron oxide abundances are not considered for simplicity. The full list of parameters used for these calculations are listed in Table 3.

other compaction processes using the measured densities of extant asteroids. It has also been difficult to use spectral observations for this purpose because the various chondrite petrologic types have generally similar absorption spectra (Gaffey et al., 1993b). For example, spectral variations among C, G, B, and F-type asteroids have been attributed to metamorphic heating (Hiroi et al., 1996), but the presence of absorption features from hydrated minerals complicates this interpretation (Vilas and Sykes, 1996).

Lutetia's high bulk density provides clear evidence for the effects of early compaction processes. The asteroid's density equals or exceeds the mean bulk densities of all known sintered chondrite groups (e.g., enstatite, ordinary, and carbonaceous chondrites other than CB chondrites) and far exceeds that of weakly heated chondrites (CI1 and CM2 groups). This makes it the first well-characterized asteroid to directly reflect the early metamorphic, sintering, impact and other compaction processes, which have until now been mainly inferred from meteorites.

4.2. Possible evidence for a differentiated interior

Even if Lutetia has 0% macroporosity, its density would exceed the mean densities of all known non-CB, –CH, and –CR carbonaceous chondrite groups. Therefore, if Lutetia initially was composed completely of undifferentiated non-CB, –CH, and –CR carbonaceous chondritic materials, its interior would likely need to have melted and formed a metallic core as described in more detail below. By comparison, if Lutetia were initially completely composed of enstatite chondrite materials, interior differentiation would only be indicated for $>13\%$ macroporosity. Given the qualitative evidence presented in Section 3 that Lutetia's macroporosity likely exceeds 13%, Lutetia's bulk density implies that if it initially had a non-CB, –CH, and –CR carbonaceous chondrite bulk composition, its interior is certainly differentiated, while if it had initially an enstatite chondrite bulk composition, indicate interior differentiation is likely but not required.

Although melting alone mostly redistributes elements throughout the body without leading to substantial bulk density changes, differentiation leading to the formation of a metallic core could have increased the bulk density of Lutetia relative to that of the sintered, unmelted state through at least two effects. Firstly, measurements of meteorites indicate that melting usually leads to a further reduction of porosity: iron and stony iron meteorites have near-zero bulk porosity, basaltic achondrite groups have $\sim$3–14% mean porosities, while as discussed in Section 4.1, sintered chondrite groups have mean porosities ranging from $\sim$7–25% (Consolmagno et al., 2008). To quantify the implications of this for the bulk density of Lutetia, we estimated the bulk density of a Lutetia-sized spherical asteroid subject to post-accretional heating (from the decay of short-lived nuclides such as ^{26}Al). Such bodies melt from the inside outward (Hevey and Sanders, 2006; Sahijpal et al., 2007) and therefore may retain an unmelted chondritic crust of variable thickness (Elkins-Tanton et al., 2011) (Figs. 3, 4A). If the body accretes instantaneously before $\sim$0.8–1.5 Ma after the formation of CAIs, internal temperatures would reach the solidus of the constituent silicates ($\sim$1200 °C). Under these conditions, we assume a central metallic core could form quickly beneath the silicate magma ocean in a body of Lutetia's size [see Sahijpal et al. (2007)]. For instantaneous accretion, only a thin ($\ll$1 km thick) unmelted but mostly sintered chondritic crust may be retained (Elkins-Tanton et al., 2011), but if the body continuously accreted beginning before $\sim$1.5 Ma after the formation of CAIs and extending over several Ma, it could build up a substantial (potentially many km thick) unmelted crust.

Sintered chondrite (~7-25% porosity)

Basaltic achondrite (~5% porosity)
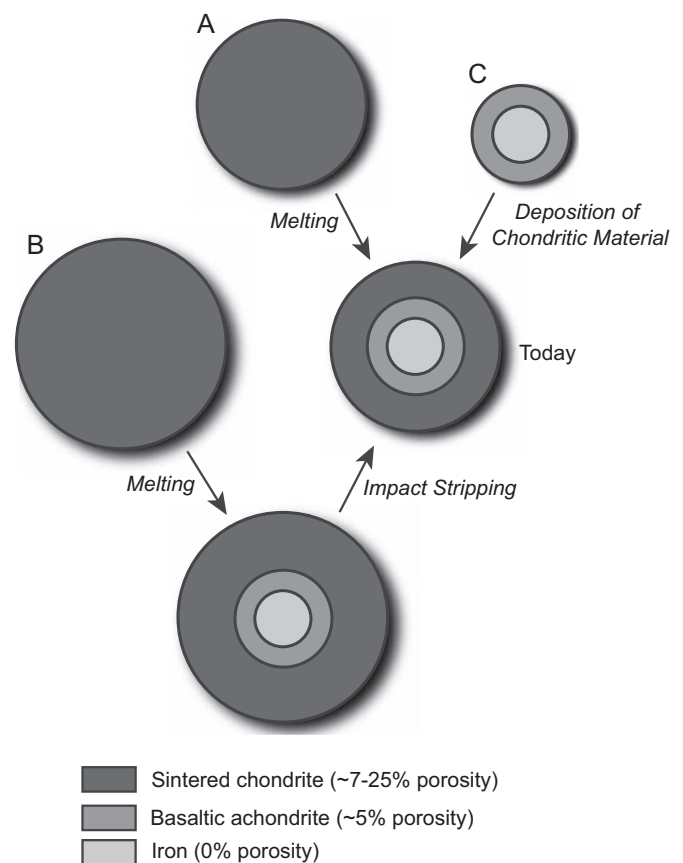
Iron (0% porosity)

Fig. 4. Three end-member scenarios that could produce the high bulk density of Lutetia via formation of a partially differentiated body. (A) Proto-Lutetia had nearly the same radius as present Lutetia but was initially undifferentiated (dark gray). Subsequent melting of the interior formed a metallic core (light gray) and silicate mantle (medium gray), decreasing the bulk porosity and therefore increasing the bulk density. (B) Proto-Lutetia was undifferentiated and had a larger radius than present-day Lutetia. A smaller volume fraction of this body experienced melting than the body in (A). Subsequent impacts removed much of the undifferentiated outer layer, thereby increasing the bulk density. (C) Proto-Lutetia differentiated early and either did not initially retain a chondritic crust or else lost such an early crust by early impact stripping. An outer layer of chondritic debris was subsequently deposited on the body. This figure is schematic and the layer thicknesses are not drawn to scale.

We estimated the bulk density of these bodies using measurements of meteorites representing the expected lithology for the core, melted silicate mantle and primordial chondritic crust (iron meteorite, basaltic achondrites, and a wide variety of chondrite groups, respectively). We find that if Lutetia has a bulk metal abundance like that of nearly all known chondrites [<15 vol% mean value for all groups except for the rare CB and CH chondrites (Scott and Krot, 2005)], a sintered but unmelted crust with densities similar to chondrites of petrologic type ≥ 3, and nominal 20% macroporosity throughout, more than $\sim$80% of the body's radius would be required to have melted in order to explain Lutetia's high density (Fig. 3B). Given that the lack of bedrock of exposures of differentiated interior rocks indicates a minimum several km thickness for the chondritic crust, a body with a sintered crust and the latter metal abundance could have a maximum macroporosity of $\sim$25% (Fig. 3B). Even a larger fraction of a body with a porous, unsintered crust and the same metal abundance would have to be melted (Fig. 3A). Alternatively, if we consider a metal abundance at the upper end of the range of non-CB and –CH carbonaceous chondrite groups ($\sim$5 vol%), then even a body with a sintered crust and macroporosity of just $\sim$9% would also require melting out to 80% of the body radius (Fig. 3B).

The second way the bulk density could be increased relative to the unmelted state is by the removal of the relatively low density silicate crust by hypervelocity impacts below the catastrophic disruption threshold (Holsapple, 2009). Because the present radius of Lutetia is fixed, this would be roughly equivalent to having formed a body with larger radius than that presently observed, which was subsequently reduced to the present radius through removal (thinning) of its chondritic crust (Fig. 4B). Assuming this material is removed uniformly around the body without excavation of the differentiated interior, this is equivalent to a body with fixed present radius but with a thinner unmelted crust (more interior melting) (i.e., moving to a new curve to the right in Fig. 3). This would reduce the fraction of the original body that must have melted to explain the density described above, but would not change the requirement that 80% of the present radius must be melted. An extreme end member of this scenario, motivated by hit-and-run models for the formation of the IVA iron meteorite parent body (Asphaug, 2010), is complete removal of much or all of the silicate exterior (including any chondritic crust and possibly some of the differentiated silicate mantle) followed by deposition of a veneer of chondritic material (which would be equivalent to both moving both to a new curve and to a higher metal abundance in Fig. 3) (Fig. 4C). It is also conceivable that a fully differentiated body could be covered by chondritic material from a foreign impactor (Fig. 4C). Notably, because thermal models indicate that the unmelted chondritic crust could range in thickness up to tens of km (Elkins-Tanton et al., 2011), the impact craters now visible on Lutetia need not have penetrated the crust into the melted interior.

5. Conclusions

Lutetia's high density and surface composition indicate that it has much lower porosity than that inferred for primordial fluffy accretional aggregates. This provides evidence for the action of sintering by postulated planetary heat sources (e.g., short-lived radionuclides) and impact-induced compaction. These asteroidal compaction processes have until now been inferred from the varied petrologic types (3–7) of chondrite groups (Huss et al., 2006) rather than from direct observations asteroids.

If Lutetia even has $> \sim 13\%$ macroporosity, a value modest for asteroids of Lutetia's size and consistent with indications that it is thoroughly fractured, then it likely has a melted interior including a metallic core or at least large, metal-rich regions. Such a partially differentiated structure is predicted to be a natural outgrowth of prolonged accretion beginning before 1.5 Ma and extending for several Ma (Elkins-Tanton et al., 2011; Sahijpal and Gupta, 2011). This structure might also result from a scenario in which chondrules formed via the collisions of molten planetesimals and then accreted onto the surfaces of the colliding bodies (Asphaug et al., 2011) (a variant on scenario pictured in Fig. 4C). Previously, candidate partially melted asteroids have been tentatively identified based on spectral evidence, but density data for these objects do not suggest metallic core formation on these bodies [e.g., (Abell et al., 2007; McCoy et al., 2001)]. Partial differentiation and core formation on Lutetia would be consistent with the proposal that some chondrites and achondrites could have a common parent body origin, and also support recent arguments that the remanent magnetization observed in some metamorphosed carbonaceous chondrites could be the product of an internal core dynamo rather than the early nebula or sun (Carporzen et al., 2011; Elkins-Tanton et al., 2011; Weiss et al., 2010). It would further suggest that some asteroids whose surfaces are chondritic may in fact be partially differentiated, concealing an interior metallic core.

References

Abell, P.A., Vilas, F., Jarvis, K.S., Gaffey, M.J., Kelley, M.S., 2007. Mineralogical composition of (25143) Itokawa 1998 SF36 from visible and near-infrared reflectance spectroscopy: Evidence for partial melting. Meteoritics and Planetary Science 42, 2165–2177.

Anders, E., 1964. Origin, age, and composition of meteorites. Space Science Reviews 3, 583–714.

Asphaug, E., Moore, J.M., Morrison, D., Benz, W., Nolan, M.C., Sullivan, R.J., 1996. Mechanical and geological effects of impact cratering on Ida. Icarus 120, 158–184.

Asphaug, E., Ryan, E.V., Zuber, M.T., 2002. Asteroid interiors. In: Bottke, W.F., Cellino, A., Paolicchi, P., Binzel, R.P. (Eds.), Asteroids III, pp. 463–484.

Asphaug, E., 2009. Growth and evolution of asteroids. Annual Review of Earth and Planetary Science 37, 413–448.

Asphaug, E., 2010. Similar-sized collisions and the diversity of planets. Chemie der Erde 70, 199–219.

Asphaug, E., Jutzi, M., Movshovitz, N., 2011. Chondrule formation during planetesimal accretion. Earth and Planetary Science Letters 308, 369–379.

Auster, H.U., Richter, I., Glassmeier, K.-H., Berghofer, G., Carr, C.M., Motschmann, U., 2010. Magnetic field investigations during ROSETTA's 2867 Šteins flyby. Planetary and Space Science 58, 1124–1128.

Barucci, M.A., Fornasier, S., Dotto, E., Lamy, P.L., Jorda, L., Groussin, O., Brucato, J.R., Carvano, J., Alvarez-Candal, A., Cruikshank, D., Fulchignoni, M., 2008. Asteroids 2867 Steins and 21 Lutetia: surface composition from far infrared observations with the Spitzer space telescope. Astronomy and Astrophysics 477, 665–670.

Barucci, M.A., Fulchignoni, M., 2009. Pre-fly-by properties of the Rosetta asteroids targets 2867 Steins and 21 Lutetia. In: Schulz, R., Alexander, C., Boenhardt, H., Glassmeier, K.-H. (Eds.), Rosetta: ESA's Mission to the Origin of the Solar System, Springer, pp. 55–68.

Baumgartel, K., Sauer, K., Story, T.R., McKenzie, J.F., 2007. Solar wind response to a magnetized asteroid: Linear theory. Icarus 129, 94–105.

Belskaya, I.N., Fornasier, S., Krugly, Y.N., Shevchenko, V.G., Gaftonyuk, N.M., Barucci, M.A., Fulchignoni, M., Gil-Hutton, R., 2010. Puzzling asteroid 21 Lutetia: Our knowledge prior to the Rosetta fly-by. Astronomy and Astrophysics, 515. doi:10.1051/0004-6361/201013994.

Benz, W., Asphaug, E., 1999. Catastrophic disruptions revisited. Icarus 142, 5–20.

Birlan, M., Vernazza, P., Fulchignoni, M., Barucci, M.A., Descamps, P., Binzel, R.P., Bus, S.J., 2006. Near infra-red spectroscopy of the asteroid 21 Lutetia: I. New results of long-term campaign. Astronomy and Astrophysics 454, 677–681.

Bland, P.A., Howard, L.E., Prior, D.J., Wheeler, J., Hough, R.M., Dyl, K.A., 2011. Earliest rock fabric formed in the Solar System preserved in a chondrule rim. Nature Geoscience 4, 244–247.

Bottke, W.F., Durda, D.D., Nesvorný, D., Jedicke, R., Morbidelli, A., Vokrouhlický, D., Levison, H., 2005. The fossilized size distribution of the main asteroid belt. Icarus 175, 111–140.

Bottke, W.F., Nesvorný, D., Grimm, R.E., Morbidelli, A., O'Brien, D.P., 2006. Iron meteorites as remnants of planetesimals formed in the terrestrial planet region. Nature 439, 821–824.

Brearley, A.J., 2006. The action of water. In: Lauretta, D.S., McSween, H.Y. (Eds.), Meteorites and the Early Solar System II, University of Arizona Press, Tucson, pp. 587–624.

Britt, D., Consolmagno, G.J., 2003. Stony meteorite porosities and densities: A review of the data through 2001. Meteoritics and Planetary Science 38, 1161–1180.

Britt, D.T., Yeomans, D.K., Housen, K., Consolmagno, G., 2002. Asteroid density, porosity, and structure. In: Bottke, W.F., Cellino, A., Paolicchi, P., Binzel, R.P. (Eds.), Asteroids III, University of Arizona Press, Tucson, pp. 485–500.

Burbine, T.H., McCoy, T.J., Meibom, A., Gladman, B., Keil, K., 2002. Meteoritic parent bodies: Their number and identification. In: Bottke, W.F., Cellino, A., Paolicchi, P., Binzel, R.P. (Eds.), Asteroids III, University of Arizona Press, Tucson, pp. 653–667.

Carporzen, L., Weiss, B.P., Elkins-Tanton, L.T., Shuster, D.L., Ebel, D.S., Gattacceca, J., 2011. Magnetic evidence for a partially differentiated carbonaceous chondrite parent body. Proceedings of the National academy of Sciences of the United States of America 108, 6386–6389.

Chapman, C.R., Salisbury, J.W., 1973. Comparisons of meteorite and asteroid spectral reflectivities. Icarus 19, 507–522.

Clark, B.E., Hapke, B., Pieters, C., Britt, D., 2002. Asteroid space weathering and regolith evolution. In: Bottke, W.F., Cellino, A., Paolicchi, P., Binzel, R.P. (Eds.), Asteroids III, University of Arizona Press, Tucson, pp. 585–599.

Clark, B.E., Ockert-Bell, M.E., Cloutis, E.A., Nesvorny, D., Mothe-Diniz, T., Bus, S.J., 2009. Spectroscopy of K-complex asteroids: Parent bodies of carbonaceous meteorites? Icarus 202, 119–133.

Cloutis, E.A., Hardersen, P.R., Bish, D.L., Bailey, D.T., Gaffey, M.J., Craig, M.A., 2010. Reflectance spectra of iron meteorites: Implications for spectral identification of their parent bodies. Meteoritics and Planetary Science 45, 304–332.

Cody, G.D., Alexander, C.M.O.D., Yabuta, H., Kilcoyne, A.L.D., Araki, T., Ade, H., Dera, P., Fogel, M., Militzer, B., Mysen, B.O., 2008. Organic thermometry for chondritic parent bodies. Earth and Planetary Science Letters 272, 446–455.

Consolmagno, G.J., Britt, D.T., 2004. Meteoritical evidence and constraints on asteroid impacts and disruption. Planetary and Space Science 52, 1119–1128.

Consolmagno, G.J., Wignarajah, D.P., Britt, D.T., 2007. Bulk densities of assorted CK chondrites, primitive achondrites, and Bencubbin. Proceedings of the 70th Annual Meeting of the Meteoritical Society: Abstract #5118.

Consolmagno, G.J., Britt, D.J., Macke, R.J., 2008. The significance of meteorite density and porosity. Chemie der Erde 68, 1–29.

Coradini, A., Coradini, A., Coradini, A., Coradini, A., Coradini, A., Coradini, A., 2011. Rosetta composition paper. Science, in press.

Davis, D.R., 1999. The collisional history of asteroid 253 Mathilde. Icarus 140, 49–52.

Davison, T.M., Collins, G.S., Ciesla, F.J., 2010. Numerical modelling of heating in porous planetesimal collisions. Icarus 208, 468–481.

Decamps, P., Marchis, F., Pollock, J., Berthier, J., Vachier, F., Birlan, M., Kaasalainen, M., Harris, A.W., Wong, M.H., Romanishin, W.J., Cooper, E.M., Kettner, K.A., Wiggins, P., Kryszczynska, A., Polinska, M., Coliac, J.-F., Devyatkink, V., Verestchagina, I., Gorshanov, D., 2008. New determination of the size and bulk density of the binary asteroid 22 Kalliope from observations of mutual eclipses. Icarus 196, 578–600.

Demeo, F.E., Binzel, R.P., Slivan, S.M., Bus, S.J., 2009. An extension of the Bus asteroid taxonomy into the infrared. Icarus 202, 160–180.

Drummond, J.A., Conrad, A., Merline, W.J., Carry, B., Chapman, C.R., Weaver, H.A., Tamblyn, P.M., Christou, J.C., Dumas, C., 2010. Physical properties of the ESA Rosetta target asteroid (21) Lutetia. I. The triaxial ellipsoid dimensions, rotational pole, and bulk density Lutetia. Astronomy and Astrophysics, 523. doi:10.1051/0004-6361/201015075.

Dyar, M.D., Treiman, A.H., Pieters, C.M., Hiroi, T., Lane, M.D., O'Connor, V., 2005. MIL03346, the most oxidized Martian meteorite: A first look at spectroscopy, petrography, and mineral chemistry. Journal of Geophysical Research, 110. doi:10.1029/2005JE002426.

Elkins-Tanton, L.T., Weiss, B.P., Zuber, M.T., 2011. Chondrites as samples of differentiated planetesimals. Earth and Planetary Science Letters 305, 1–10.

Flynn, G.J., 1994. Interplanetary dust particles collected from the stratosphere: Physical, chemical, and mineralogical properties and implications for their sources. Planetary and Space Science 42, 1151–1161.

Gaffey, M.J., 1976. Spectral reflectance characteristics of the meteorite classes. Journal of Geophysical Research 81, 905–920.

Gaffey, M.J., Bell, J.F., Brown, R.H., Burbine, T.H., Piatek, J.L., Reed, K.L., Chaky, D.A., 1993a. Mineralogical variations within the S-type asteroid class. Icarus 106, 573–602.

Gaffey, M.J., Burbine, T.H., Binzel, R.P., 1993b. Asteroid spectroscopy: Progress and perspectives. Meteoritics 28, 161–187.

Geake, J.E., Dollfus, A., 1986. Planetary surface texture and albedo from parameter plots of optical polarization data. Monthy Notices of the Royal Astronomical Society 218, 75–91.

Ghosh, A., Weidenschilling, S.J., McSween, H.Y., Rubin, A.E., 2006. Asteroidal heating and thermal stratification of the asteroid belt. In: Lauretta, D.S., McSween, H.Y. (Eds.), Meteorites and the Early Solar System II, University of Arizona Press, Tucson, pp. 555–556.

Gilbert, G.K., 1893. The Moon's face: A study of the origin of its features. Philosophical Society of Washington Bulletin 12, 241–292.

Gulkis, S., Keihm, S., Kamp, L., Lee, S., Hartogh, P., Crovisier, J., 2011. Continuum and spectroscopic observations of asteroid (21) Lutetia at millimeter and submillimeter wavelengths with the MIRO instrument on the Rosetta spacecraft. Planetary and Space Science, Submitted for publication.

Hevey, P.J., Sanders, I.S., 2006. A model for planetesimal meltdown by ^{26}Al and its implications for meteorite parent bodies. Meteoritics and Planetary Science 41, 95–106.

Hiroi, T., Takeda, H., 1991. Reflectance spectroscopy and mineralogy of primitive achondrites-lodranites. Proceedings of the NIPR Symposium on Antarctic Meteorites 4, 163–177.

Hiroi, T., Bell, J.F., Takeda, H., Pieters, C., 1993. Spectral comparison between olivine-rich asteroids and pallasites. Proceedings of the NIPR Symposium on Antarctic Meteorites 6, 234–245.

Hiroi, T., Zolensky, M.E., Pieters, C.M., Lipschutz, M.E., 1996. Thermal metamorphism of the C, G, B, and F asteroids seen from the 0.7 p.1m, 3 p.1m, and UV absorption strengths in comparison with carbonaceous chondrites. Meteoritics and Planetary Science 31 (321–327).

Holsapple, K., Giblin, I., Housen, K., Nakamura, A.M., Ryan, E., 2002. Asteroid impacts: Laboratory experiments and scaling laws. In: Bottke, W.F., Cellino, A.,

Paolicchi, R.P., Binzel, R.P. (Eds.), Asteroids III, University of Arizona Press, Tucson, pp. 443–462.

Holsapple, K., 2009. On the"strength"of the small bodies of the solar system: A review of strength theories and their implementation for analyses of impact disruptions. Planetary and Space Science 57, 127–141.

Holsapple, K.A., Housen, K.R., 2007. A crater and its ejecta: An interpretation of Deep Impact. Icarus 187, 345–356.

Housen, K., 2009. Cumulative damage in strength-dominated collisions of rocky asteroids: Rubble piles and brick piles. Planetary and Space Science 57, 142–153.

Housen, K.R., Holsapple, K.A., 2003. Impact cratering on porous asteroids. Icarus 163, 102–119.

Huss, G.R., Rubin, A.E., Grossman, J.N., 2006. Thermal metamorphism in chondrites. In: Lauretta, D.S., McSween, H.Y. (Eds.), Meteorites and the Early Solar System II, University of Arizona Press, Tucson, pp. 567–586.

Izawa, M.R.M., King, P.L., Flemming, R.L., Peterson, R.C., McCausland, P.J.A., 2010. Mineralogical and spectroscopic investigation of enstatite chondrites by X-ray diffraction and infrared reflectance spectroscopy. Journal of Geophysical Research 115, E07008. doi:07010.01029/02009JE003452.

Keil, K., Stöffler, D., Love, S.G., Scott, E.R.D., 1997. Constraints on the role of impact heating and melting in asteroids. Meteoritics and Planetary Science 32, 349–363.

Kuzmanoski, M., Apostolovska, G., Novaković, B., 2010. The mass of (4) Vesta derived from its largest gravitational effects. Astronomical Journal 140, 880–886.

Lazzarin, M., Marchi, S., Moroz, L.V., Magrin, S., 2009. New visible spectra and mineralogical assessment of (21) Lutetia, a target of the Rosetta mission. Astronomy and Astrophysics 498, 307–311.

Lupishko, D.F., Belskaya, I.N., 1989. On the surface composition of the M-type asteroids. Icarus 78, 395–401.

Macke, R.J., Consolmagno, G.J., Britt, D.T., Huston, M.L., 2010. Enstatite chondrite density, magnetic susceptibility, and porosity. Meteoritics and Planetary Science 45, 1513–1526.

Magri, C., Nolan, M.C., Ostro, S.J., Giorgini, J.D., 1997. A radar survey of main-belt asteroids: Arecibo observations of 55 objects during 1999–2003. Icarus 186, 126–151.

Marchi, S., Paolicchi, P., Lazzarin, M., Magrin, S., 2006. A general spectral slope-exposure relation for S-type main belt and near-earth asteroids. Astronomical Journal 131, 1138–1141.

Marchi, S., Barbieri, C., Küppers, M., Marzari, F., Davidsson, B., Keller, H.U., Besse, S., Lamy, P.L., Mottola, S., Massironi, M., Cremonese, G., 2010. The cratering history of asteroid (2867) Steins. Planetary and Space Science 58, 1116–1123.

Marchi, S., Massironi, M., Vincent, J.-B., Morbidelli, A., Mottola, S., Marzari, F., Küppers, M., Besse, S., Thomas, N., Barbieri, C., Naletto, G., Sierks, H., 2010. The cratering history of asteroid (21) Lutetia. Planetary and Space Science, in press.

McCoy, T.J., Burbine, T.H., McFadden, L.A., Starr, R.D., Gaffey, M.J., Nittler, L.R., Evans, L.G., Izenburg, N., Lucey, P.G., Trombka, J.I., Bell, J.F., Clark, B.E., Clark, P.E., Squyres, S.W., Chapman, C.R., Boynton, W.V., Veverka, J., 2001. The composition of 433 Eros: A mineralogical-chemical synthesis. Meteoritics and Planetary Science 36, 1661–1672.

McSween, H.Y., Ghosh, A., Grimm, R.E., Wilson, L, Young, E.D., 2002. Thermal evolution models of asteroids. In: Bottke, W.F., Cellino, A., Paolicchi, P., Binzel, R.P. (Eds.), Asteroids III, University of Arizona Press, Tucson, pp. 559–571.

Ockert-Bell, M.E., Clark, B.E.S., Isaacs, M.E., Cloutis, R.A., Fornasier, E.A., Bus, S.J., S., 2010. The composition of M-type asteroids: Synthesis of spectroscopic and radar observations. Icarus 210, 674–692.

Osawa, T., Kagi, H., Nakamura, T., Noguchi, T., 2005. Infrared spectroscopic taxonomy for carbonaceous chondrites from speciation of hydrous components. Meteoritics and Planetary Science 40, 71–86.

Pätzold, M., Andert, T.P., Asmar, S.W., Anderson, J.D., Barriot, J.-P., Bird, M.K., Häusler, B., Hahn, M., Tellmann, S., Sierks, H., Lamy, P., Weiss, B.P., 2011. Asteroid (21) Lutetia – low mass, high density. Science, in press.

Petrovic, J.J., 2001. Mechanical properties of meteorites and their constitutents. Journal of Materials Science 36, 1579–1583.

Pieters, C.M., Klima, R.L., Hiroi, T., Dyar, M.D., Lane, M.D., Treiman, A.H., Noble, S.K., Sunshine, J.M., Bishop, J.L., 2008. Martian dunite NWA 2737: Integrated spectroscopic analyses of brown olivine. Journal of Geophysical Research, 113. doi:10.1029/2007JE002939.

Richter, I., Auster, H.U., Glassmeier, K.-H., Koenders, C., Carr, C.M., Motschmann, U., Muller, J., McKenna-Lawlor, S. 2011. Magnetic field investigations during the Rosetta flyby at asteroid (21) Lutetia. Planetary and Space Science, doi: 10.1016/j.pss.2011.08.009. In press.

Rivkin, A.S., Clark, B.E., Ockert-Bell, M.E., Shepard, M.K., Volquardsen, E.L., Howell, E.S., Bus, S.J., 2011. Observations of 21 Lutetia in the 2–4 μm region with the NASA IRTF. Lunar and Planetary Science Conference XLII abstract #1439.

Rubin, A.E., 2004. Postshock annealing and postannealing shock in equilibrated ordinary chondrites: Implications for the thermal and shock histories of chondritic asteroids. Geochimica et Cosmochimica Acta 68, 673–689.

Runcorn, S.K., 1975. On the interpretation of lunar magnetism. Physics of the Earth and Planetary Interiors 10, 327–335.

Ryan, E.V., Melosh, H.J., 1998. Impact fragmentation: From the laboratory to asteroids. Icarus 133, 1–24.

Sahijpal, S., Soni, P., Gupta, G., 2007. Numerical simulations of the differentiation of accreting planetesimals with ^{26}Al and ^{60}Fe as the heat sources. Meteoritics and Planetary Science 42, 1529–1548.

Sahijpal, S., Gupta, G., 2011. Did the carbonaceous chondrites evolve in the crustal regions of partially differentiated asteroids? Journal of Geophysical Research, 116. doi:10.1029/2010JE003757.

Salisbury, J.W., D'Aria, D.M., Jarosewich, E., 1991. Midinfrared (2.5–13.5 μm) reflectance spectra of powdered stony meteorites. Icarus 92, 280–297.

Scott, E.R.D., Krot, A.N., 2005. Chondritic meteorites and the high-temperature nebular origins of their components. In: Krot, A.N., Scott, E.R.D., Reipurth, B. (Eds.), Chondrites and the Protoplanetary Disk, 341. , ASP Conference Series, pp. 15–53.

Shepard, M.K., Clark, B.E., Ockert-Bell, M., Nolan, M.C., Howell, E.S., Magri, C., Giorgini, J.D., Benner, L.A.M., Ostro, S.J., Harris, A.W., Warner, J.L., Stephens, R.D., Mueller, M., 2010. A radar survey of M- and X-class asteroids II. Summary and synthesis. Icarus 208, 221–237.

Sierks, H., Lamy, P., Barbieri, C., Koschny, D., Rickman, H., Rodrigo, R., A'Hearn, M.F.A., Angrilli, F., Barucci, M.A., Bertaux, J.-L., Bertini, I., Besse, S., Carry, B., Cremonese, G., Da Deppo, V., Davidsson, B., Debei, S., De Cecco, M., De Leon, J., Ferri, F., Fornasier, S., Fulle, M., Hviid, S.F., Gaskell, R.W., Groussin, O., Gutierrez, P., Ip, W., Jorda, L., Kaasalainen, M., Keller, H.U., Knollenberg, J., Kramm, R., Kührt, E., Küppers, M., Lara, L., Leyrat, C., Lazzarin, M., Lopez Moreno, J.J., Magrin, S., Marchi, S., Marzari, F., Massironi, M., Michalik, H., Moissl, R., Naletto, G., Preusker, F., Sabau, L., Sabolo, W., Scholten, F., Snodgrass, C., Thomas, N., Tubiana, C., Vernazza, P., Vincent, J.-B., Wenzel, K.-P., Andert, T., Pätzold, M., Weiss, B.P., 2011. Images of asteroid 21 Lutetia: A remnant planetesimal from the early solar system. Science, in press.

Simon, S., Bagdonat, T., Motschmann, U., Glassmeier, K.-H., 2006. Plasma environment of magnetized asteroids: a 3-D hybrid simulation study. Annales Geophysicae 24, 407–414.

Sugiura, N., Strangway, D.W., 1983. Magnetic anisotropy and porosity of chondrites. Geophysical Research Letters 10, 83–86.

Svetsov, V.V., Nemtchinov, I.V., Teterev, A.V., 1995. Disintegration of large meteoroids in Earth's atmosphere: theoretical models. Icarus 116, 131–153.

Thomas, P.C., Belton, M.J.S., Carcich, B., Chapman, C.R., Davies, M.E., Sullivan, R., Veverka, J., 1996. The shape of Ida. Icarus 120, 20–32.

Tsuchiyama, A., Mashio, E., Imai, Y., Noguchi, T., Miura, Y.N., Yano, H., 1998. In: Proceedings of the Japan Geoscience Union Meeting 2008, Abstract #P168.

Vernazza, P., Brunetto, R., Binzel, R.P., Perron, C., Fulvio, D., Strazzulla, G., Fulchignoni, M., 2009. Plausible parent bodies for enstatite chondrites and mesosiderites: Implications for Lutetia's fly-by. Icarus 202, 477–486.

Veverka, J., Thomas, P., Harch, A., Clark, B., Bell, J.F., Carcich, B., Joseph, J., Chapman, C., Merline, W., Robinson, M., Malin, M., McFadden, L.A., Murchie, S., Hawkins, S.E., Farquhar, R., Izenberg, N., Cheng, A., 1997. NEAR's flyby of 253 Mathilde: Images of a C asteroid. Science 278, 2709–2714.

Vilas, F., Sykes, M.V., 1996. Are low-albedo asteroids thermally metamorphosed? Icarus 124, 483–489.

Weidenschilling, S.J., Cuzzi, J.N., 2006. Accretion dynamics and timescales: Relation to chondrites. In: Lauretta, D.S., McSween, H.Y. (Eds.), Meteorites and the Early Solar System II, University of Arizona Press, Tucson, pp. 473–485.

Weiss, B.P., Berdahl, S., Elkins-Tanton, L.T., Stanley, S., Lima, E.A., Carporzen, L., 2008. Magnetism on the angrite parent body and the early differentiation of planetesimals. Science 322, 713–716.

Weiss, B.P., Gattacceca, J., Stanley, S., Rochette, P., Christensen, U.R., 2010. Paleomagnetic records of meteorites and early planetesimal differentiation. Space Science Reviews 152, 341–390.

Wilkison, S.L., Robinson, M.S., Thomas, P.C., Veverka, J., McCoy, T.J., Murchie, S.L., Prockter, L.M., 2002. An estimate of Eros's porosity and implications for internal structure. Icarus 155, 94–103.

Yomogida, K., Takafumi, M., 1983. Physical properties of ordinary chondrites. Journal of Geophysical Research 88, 9513–9533.

Yomogida, K., Matsui, T., 1984. Multiple parent bodies of ordinary chondrites. Earth and Planetary Science Letters 68, 34–42.